GRAIN BOUNDARY CORROSION AND ALTERATION PHASE FORMATION DURING THE OXIDATIVE DISSOLUTION OF UO$_2$ PELLETS

RECEIVED
FEB 20 1997
OSTI

D. J. Wronkiewicz, E. C. Buck, and J. K. Bates

ARGONNE NATIONAL LABORATORY
Chemical Technology Division
9700 South Cass Avenue
Argonne, IL 60439-4837

MASTER

Submitted to

DISCLAIMER

**Portions of this document may be illegible
in electronic image products. Images are
produced from the best available original
document.**

GRAIN BOUNDARY CORROSION AND ALTERATION PHASE FORMATION DURING THE OXIDATIVE DISSOLUTION OF UO$_2$ PELLETS

David J. Wronkiewicz, Edgar C. Buck, and John K. Bates
Argonne National Laboratory, Argonne, IL 60439-4837, USA, wronkiewicz@cmt.anl.gov

ABSTRACT

The alteration behavior of UO$_2$ pellets following their reaction under unsaturated drip-test conditions, at 90°C, for time periods of up to 10 years has been examined by solid phase and leachate analyses. Sample reactions were characterized by preferential dissolution of grain boundaries between the original press-sintered UO$_2$ granules comprising the samples, development of a polygonal network of open channels along the intergrain boundaries, and spallation of surface granules that had undergone severe grain boundary corrosion. The development of a dense mat of alteration phases after two years of reaction trapped loose granules, resulting in reduced rates of particulate uranium release. The paragenetic sequence of alteration phases that formed on the present samples was similar to that observed in surficial weathering zones of natural uraninite (UO$_2$) deposits, with alkali and alkaline earth uranyl silicates representing the long-term solubility-limiting phases for uranium in both systems.

INTRODUCTION

The dissolution of spent nuclear fuel from commercial power reactors represents the largest potential source of radionuclide release from high-level waste forms in a disposal vault because of the large volumes of spent fuel that need to be disposed and the high concentration of radionuclides contained in the spent fuel rods. Nearly 30,000 metric tons of commercial spent nuclear fuel were in storage at commercial power reactors as of 1995, while future projections suggest that this quantity will more than double by the anticipated opening of the potential Yucca Mountain, Nevada high-level nuclear waste repository in 2010 [1]. Consequently, the dissolution behavior of the spent fuel (irradiated UO$_2$), and the rates and mechanisms of radionuclide release are critical parameters that will need to be determined before the performance of a nuclear waste repository containing spent fuel can be assessed.

The oxidation of UO$_2$ leads to the formation of progressively higher oxidation states of uranium and an oxidized surface layer with a composition of UO$_{2+x}$ (where $0 \leq x \leq 1$). This phase is sparingly soluble under relatively reducing conditions, where the oxidation state remains below UO$_{2.33}$. Once the oxidation state reaches UO$_{2.33}$, however, uranium solubility may increase several orders of magnitude, leading to rapid dissolution of the solid [2]. The kinetics of this oxidation step may be further enhanced when the reaction at the sample surface takes place in a thin film of water that is exposed to radiation and/or an oxidizing atmosphere [3-5]. The unsaturated geologic medium at the proposed Yucca Mountain Repository Site represents such an environment, where both an oxidizing atmosphere and limited amounts of liquid water are present. This environment may therefore significantly accelerate the reaction rate of UO$_2$, and by analogy, spent nuclear fuel in an unsaturated repository setting.

The objective of this program is to evaluate the reaction of UO$_2$ pellets following their exposure to periodic drops of simulated silicate-bicarbonate groundwater in an air atmosphere at 90°C. The corrosion of the samples was monitored by examining the surficial and cross-sectioned alteration profiles, and changes in the solution composition over time. The UO$_2$ pellets may represent an effective surrogate material for investigating the behavior of commercial spent fuel because actual spent fuel is composed of ≥95 wt% UO$_2$ [5]. The temperature of the tests is also similar to the boiling point of water at Yucca Mountain (~96°C), and thus, approximates the conditions of the first potential liquid water contact with the waste form at this site. Results from these tests will be used to characterize the (1) corrosion behavior of the pellets under conditions

that simulate an unsaturated setting, (2) formation of alteration phases, and (3) serve as a pilot study for additional tests conducted with spent nuclear fuel [6].

EXPERIMENTAL

The experimental apparatus and materials used to conduct these tests have been described previously [7-9], and thus will only briefly be summarized here. The samples were fabricated and hot-press sintered from a uranium oxide powder with a natural isotopic abundance of uranium, an oxygen/metal ratio of 2.000 ± 0.002, and <70 ppm total contaminants (mostly Cl, Th, and Fe). The pellets were assembled into Zircaloy-4 metal sleeves with their upper and lower surfaces exposed and their sides enclosed by the Zircaloy. The sample assemblies were housed in reaction vessels composed of 304L stainless steel, with the Zircaloy-UO_2 pellet assembly resting on a Teflon® support stand. The test vessels were connected to a leachant injection line and placed in an oven that was maintained at a temperature of $90 \pm 2°C$. Premeasured quantities of EJ-13 silica-bicarbonate simulated groundwater solution [7-9] were injected onto the samples via the injection line at rates of either 0.075 mL every 3.5 days or 0.0375 mL every 7 days.

Periodically, the tests were interrupted to allow for collection of the accumulated leachate. Aliquots were collected for various analyses including anion, pH, carbon, and filtered uranium. After these aliquots were removed, the stainless steel vessel bottom plus the remaining leachate solution were subjected to a 10-minute acid strip in a dilute nitric acid solution. Total uranium release (including the soluble and insoluble fractions) and the concentration of other cation components were determined from this acid strip aliquot. After completion of the sampling process, the vessels and samples were reassembled to begin the next cycle.

Individual tests were periodically terminated to provide samples for studies of solid phase alteration patterns. Five tests were terminated at periods of 1.5, 2.25, 3.5, 3.5, and 8.0 years (78, 117, 183, 183, and 417 weeks, respectively), while the remaining three tests have been allowed to continue into their eleventh year of reaction. The sample surfaces, cross-sectioned samples, and/or individual alteration phases were examined by scanning electron microscopy/energy dispersive X-ray spectrometry (SEM/EDS), optical microscopy, X-ray diffraction, and transmission electron microscopy analysis. Solution aliquots were analyzed by inductively coupled plasma mass spectrometry, Dohrman carbon analysis, and ion chromatography.

RESULTS AND DISCUSSION

Solution Analysis

Uranium release during the first ten years of testing can be broken down into three different periods (Fig. 1) [8,9]; period I, the initial incubation period of low uranium release occurring for approximately the first year of sample reaction; period II, an interval of rapid uranium release, lasting between the first and second years; and period III, an extended time interval of moderate uranium release lasting up to the present 10 years of reaction.

The majority of the uranium release during the period II could be attributed to grain boundary corrosion and spallation of UO_{2+x} particles from the samples. Uranium release during this period exceeded that of thr previous and subsequent intervals combined. An examination of the sample terminated after 1.5-years of reaction revealed the presence of a highly corroded pellet surface and numerous micrometer- to submicrometer-sized anhedral UO_{2+x} particles that were both lying directly on top of the pellets (Fig. 2a) and the alteration phases that had precipitated on this surface. These particles were, however, conspicuously absent from the surfaces of samples during period III reactions. This change occurred concurrently with: (1) the development of a dense mat of alteration phases on the top surfaces of the samples; (2) a depletion in the concentration of alkalis, alkaline earths, and silicon in the leachate solution, relative to EJ-13; and (3) a reduction in total uranium release [8,9]. These patterns indicate that the mat of alteration phases acted as a trap that encapsulated and restricted the migration of spalled UO_{2+x} particles from the sample surface. The release of the UO_{2+x} particles would now be dependent on their complete dissolution or physical release from these encapsulating phases.
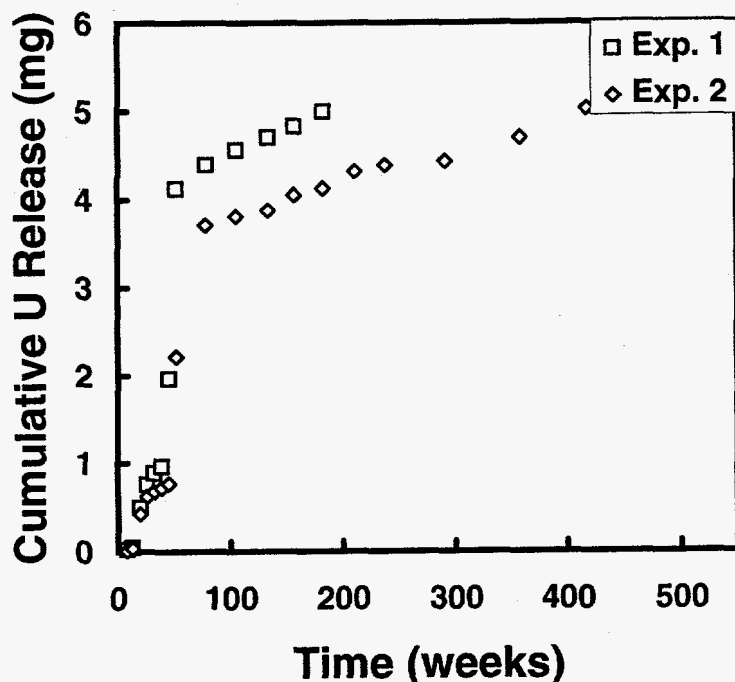
Figure 1. Cumulative release of uranium from experiments 1 and 2. Experiment 1 was terminated after 183 weeks (3.5 years), while experiment 2 was terminated after 417 weeks (8 years) of reaction. Initial pellet weights were 29,522 and 29,166 mg UO_2, respectively.

Calculated uranium release rates for period III reactions are ~0.1 to 0.3 mg/(m$^2\cdot$day) (normalized for geometric surface area). These rates represent the overall *release* of uranium, but not necessarily the true *dissolution* of uranium from the samples, since the calculated values include the added contribution of particulate uranium release, but do not include dissolved uranium that had been removed from solution through the precipitation of alteration phases.

An analysis of the size-fractioned release patterns during period III indicates that the majority (86 to 97%) of the released uranium was sorbed or precipitated on the walls of the stainless steel test vessel and the Teflon support stand. Between 1 to 12% was present as >5 nm sized particles suspended in the leachate, whereas less than 2% of the total could be attributed to components that passed through a filter with a 5-nm pore-size opening. This latter fraction

suggests a uranium concentration of 4 x 10^{-6} M for the leachate collected from the bottom of the test vessel. Electron microscopy and electron diffraction analyses of filtered residues from the eight- to ten-year leachates indicated that needle-shaped grains of uranophane and boltwoodite (Table I) were contributing to the particle release [9].

<u>Solids Analysis</u>

Examinations of the cross-sectioned samples indicate that the boundary regions between the original press-sintered UO_2 granules were preferentially dissolved relative to the cores, resulting in the formation of a polygonal network of open channels (Fig. 2b). These channels generally penetrate into the pellets to a depth of two-to-four grain boundaries (~10 to 20 mm) ahead of the exposed external sample surface. Penetration depths do, however, vary between regions displaying essentially no grain boundary corrosion to regions where penetration has occurred to a depth of approximately ten grains or more.

Spallation of UO_{2+x} surface granules was also noted in regions that had undergone severe grain boundary corrosion. This was especially prevalent on the top sample surfaces, where impact from the water droplets and also possibly flow of water across the surface had aided in the removal of loosened particles, especially during period II reactions. Loss of UO_{2+x} particles from the sample sides and bottoms appeared to be much less prevalent, whereas particle release does not appear to have occurred from the interpellet regions of the samples.
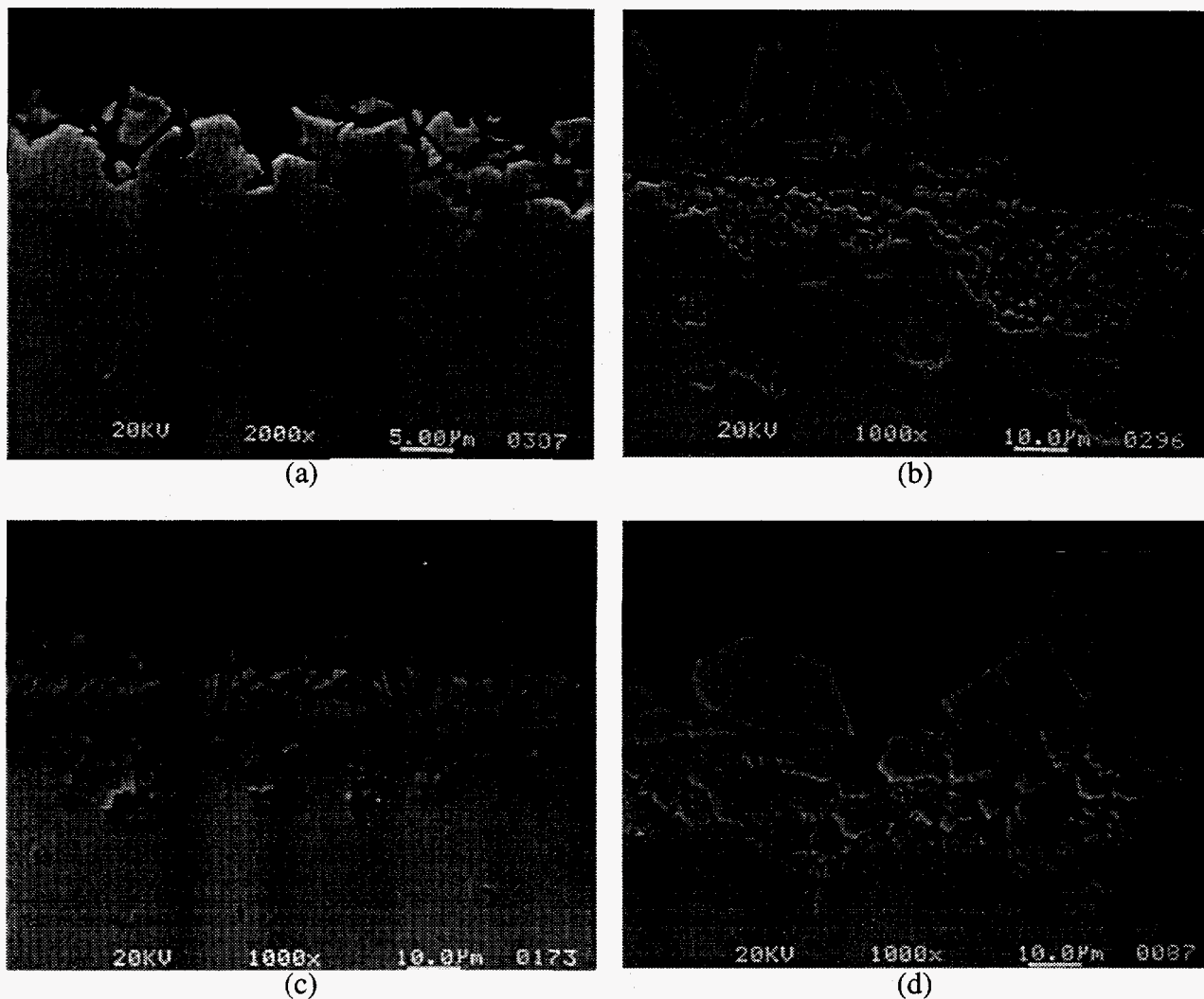
Figure 2. Scanning electron photomicrographs of cross-sectioned top surfaces of the reacted UO_2 samples. The epoxy mounting medium (black) is to the top of each photo, while the unreacted UO_2 is to the bottom. (a) 1.5-year sample displaying grain-boundary corroded surface, loosened particles, and residual pits resulting from the spallation of particles, (b) open porosity resulting from penetrative intergrannular dissolution from the 2.25-year sample. Surface layer (gray) is composed of dehydrated schoepite. Separation of layer from the pellet surface is believed to result from the contraction of the epoxy during drying. Note that the corroded UO_{2+x} surface particles have also been separated along with the alteration layer. (c) development of inner mat of compreignacite and sparse outer uranophane layer on corroded pellet surface of 3.5-year sample, (d) precipitated compreignacite on corroded top surface of 8.0-year sample. Note the continuation of crystal delamination planes from the surface phases into the open porosity region of the sample and the encapsulation of the residual UO_{2+x} surface grains by the alteration phases.

Table I. Summary of UO_2 alteration phases identified on the reacted samples

Uranyl-Oxide Hydrates

    Schoepite (meta·schoepite) $UO_3 \cdot nH_2O$ $(n < 2)$

    Dehydrated Schoepite $UO_3 \cdot (0.8 - 1.0\ H_2O)$

    Compreignacite $(Na,K)_2[(UO_2)_6O_4(OH)_6] \cdot 8\ H_2O$

    Becquerelite $Ca[(UO_2)_6O_4(OH)_6] \cdot 8\ H_2O$

Uranyl Silicate Hydrate

    Soddyite $(UO_2)_2SiO_4 \cdot 2\ H_2O$

Uranyl Alkaline Silicate Hydrates

    Uranophane $Ca(UO_2)(SiO_3)(OH)_2 \cdot 5\ H_2O$

    Boltwoodite $K_2(UO_2)_2(SiO_4)_2(H_3O)_2 \cdot H_2O$

    Na-Boltwoodite $(Na,K)(UO_2)(SiO_4)(H_3O) \cdot H_2O$

    Sklodowskite $Mg(UO_2)_2(SiO_4)_2(H_3O)_2 \cdot 2\ H_2O$

Non-Uranyl Phases

    Palygorskite $(Mg,Al_{0.12-0.66})_5(Si,Al_{0.12-0.66})_8O_{20}(OH)_5 \cdot 4\ H_2O$

    Fe-oxides

    Ti-oxides

    Amorphous silica

The sides, bottoms, and interpellet surfaces of the 3.5- and 8-year samples displayed ample evidence for intergrain boundary corrosion, though only a minimal amount of UO_{2+x} particle spallation appears to have occurred from these regions. On some of the sample bottoms, particle spallation appeared to have occurred in localized clusters, a feature suggesting that the loss of a single grain from the surface influenced the adherence of neighboring grains to the sample.

The cause for the preferential grain boundary dissolution is currently being investigated, but may be related to structural damage to the UO_2 grain-boundaries induced during the hot press-sintering process that was used to produce the pellets, electrochemical potential differences that exist along the grain boundaries, and/or density changes resulting from the partial oxidation of the uranium oxide matrix.

Oxidation from the UO_2 to the $UO_{2.25}$ state results in a slight shrinkage in unit cell dimensions [5]. This shrinkage is known to weaken the grain boundary regions in spent nuclear fuel, inducing a friable nature to the samples where light crushing or polishing caused the fuel to separate into individual grains [10,11]. Detailed backscattered electron-SEM examinations of the UO_2 samples from the present study did not reveal the presence of any density contrasts that could be associated with an increase in the oxidation state of the intergrain boundary regions. This observation suggests that any increase in oxidation state, if it occurred, either affected too small of a region to be detected at the resolution capacity of the SEM (~0.1 mm), or resulted in the rapid dissolution of any uranium that was oxidized. If the latter process occurred, then the rapid dissolution of an oxidized surface layer around the grains would suggest that the oxidation of UO_2 is the rate limiting step for the dissolution of the samples. More detailed examinations of these interpellet regions are currently being conducted to investigate this issue further.

Most of the uranium released to solution during the dissolution of the UO_2 pellets had combined with Si, Na, K, Ca, Mg, and H_2O from the EJ-13 leachant to form alteration phases. These phases precipitated on the test vessel components, sample surfaces, and within the corroded intergrain boundary regions (Figs. 2c and 2d). The end result of this process was the development

of a paragenetic sequence of alteration phases, as evident on the top surfaces of the samples, where $UO_2 \Rightarrow$ dehydrated schoepite $\Rightarrow$ compreignacite + becquerelite $\Rightarrow$ soddyite $\Rightarrow$ boltwoodite + uranophane + palygorskite clay (Table I). This trend appears to be controlled by precipitation kinetics and is nearly identical to alteration patterns observed during the weathering of naturally occurring uraninite, such as that that which occurs at the Nopal I uranium deposit in Chihuahua, Mexico [12-14]. This resemblance suggests that the conditions in the present tests have replicated an environment that may be representative of that occurring during uraninite alteration in natural oxidized systems.

The bottom of the eight-year sample displayed a relationship among the crystalline phases that is reminiscent of processes that affected the top surfaces of samples within the first few years of reaction. Dehydrated schoepite, which was the only alteration phase observed on the top surface after 1.5 years and on the bottom surface after 2.25 and 3.5 years, began to display the formation of corrosion pits at eight years [8,9]. The sharp edges of these pits suggest that a period of active dissolution was occurring when the eight-year experiment was terminated. Becquerelite and compreignacite also made their first appearance on the bottom sample surfaces at this time. This pattern is similar to that observed on the top surface after 2.25-years when becquerelite became the predominant phase by displacing the dehydrated schoepite that had formed earlier [8,9]. One may predict then, by analogy with the paragenetic sequence observed on the top sample surface, that the becquerelite that formed on the bottom surface as a replacement for dehydrated schoepite, may eventually itself be replaced by alkali and alkaline earth uranyl silicates.

Solid solution compositional changes were noted in compreignacite crystals with respect to their spatial location on the top sample surface. The molar ratio of K/Na in this phase was highest along the outside edge of the top pellet surface, where nearly pure K phases were found. The K/Na ratio decreased (down to ~0.8) down the sides of the samples, though patterns were more sporadic on the top pellet surface. These trends suggest a preference for potassium ions in the crystalline compreignacite relative to sodium (the K/Na ratio of the EJ-13 leachant is 0.17) as well as a progressive decrease of the potassium activity of the solutions as they migrate across the sample surfaces. Compreignacite was also nearly free of Ca, but did occasionally contain minor amounts of Mg. By contrast, becquerelite was identified only on the top pellet surface, and contained only minor amounts of K and Na, and no Mg. The absence of Mg was unusual in light of the common substitution of Mg for Ca in many crystalline compounds.

A cross-section examination of the samples indicated that the vast majority of the uranium released from the dissolving samples was deposited back on the surface of the UO_2 pellets and Zircaloy cladding as alteration phases (Figs. 2b-d). The quantity of uranium incorporated in these phases was calculated for the eight year sample by determining the volume of precipitated material on the sample surface, proportion of each respective alteration phase present, molar proportion of uranium contained in each phase, and multiplying the calculated volume of each phase present by its respective density. The weight of this sample prior to testing was 29,166 mg (25,709 mg of uranium). Preliminary calculations indicate that ~80 mg of uranium was incorporated into the alteration phases deposited on the sample or Zircaloy surfaces, an amount that far exceeds the 5 mg that was released from the sample-Zircaloy assembly (as recovered in the acid strip component). An additional ~780 mg of uranium remained *in situ* as undissolved UO_{2+x} cores that had undergone some corrosion along their grain boundaries.

CONCLUSIONS

Uranium release from the UO_2 samples was rapid between one and two years. The initial rapid release (period II) could be correlated with an episode of preferential dissolution along the boundaries between the UO_2 pressed grains and spallation of micrometer- to submicrometer-sized UO_{2+x} particles from the sample surfaces. Penetration along the intergrain boundaries typically occurred to a depth of two-to-four grains (~10 to 20 mm) ahead of the exposed external sample surface, but varied from regions with little visible corrosion to those where penetration occurred to a depth of approximately ten grains. Subsequent to this rapid release interval, the development of a mat of alteration phases encapsulated the loosened UO_{2+x}, resulting in a reduction of particle spallation and lower uranium release rates (period III).

Most of the uranium that was released from the samples by dissolution processes eventually precipitated back as alteration phases onto surfaces of the test components (Table I). Uranium release rates during period III, as determined from unfiltered solution aliquots, were generally between 0.1 and 0.3 mg/(m^2•day). However, less than 2% of the released uranium occurred in a soluble form (fraction that passed through a 5 nm filter). This latter value correlates to an average filtered uranium solution concentration of 4 x 10^{-6} M.

The sample reaction trends observed in the present tests closely replicated those that occur in natural geologic systems. The experiments display a sequence of phase formation that is characterized by the following paragenetic trend: UO_2 ⇒ dehydrated schoepite ⇒ compreignacite + becquerelite ⇒ soddyite ⇒ boltwoodite + uranophane + palygorskite clay. This similarity suggests that the UO_2 in the experiments has reacted by the same mechanism as uraninite in the natural deposits, and thus both the present tests and the natural analogue reactions may be used to simulate the reaction progress expected for uranium at the proposed Yucca Mountain repository. Alkali and alkaline earth uranyl silicates represent the long-term solubility-limiting phases for uranium in these systems.

The overall reaction pathway of UO_2 is controlled by a combination of factors, including oxidative-dissolution, precipitation kinetics, and leachant composition. The results from this study indicate that the alteration rates for UO_2, and by analogy, spent fuel, may be quite rapid in an unsaturated geologic setting. Alteration phases incorporated a large proportion of the uranium that was dissolved from the samples. Such a process may also act as a significant mechanism for retarding the migration of fission product and transuranic elements from spent nuclear fuel. If the effect that the uranyl phases are to have on fission product and transuranic element migration is to be included in performance assessment models, then we will need to have a greater understanding of the compositional variations of these phases, their stability at various temperatures and fluid compositions, and partition coefficient ratios that govern the incorporation of elements into their structures.

ACKNOWLEDGEMENTS

REFERENCES

1.   Integrated Data Base Report - 1994, U.S. Department of Enery Report DOE/RW-0006, Rev. 11 (1995).
2.   J. de Pablo, I. C. J. Giménez, V. Martí, and M. E. Torrero, J. Nucl. Mater. 232, 138 (1996).
3.   J. Posey-Dowty, E. Axtmann, D. Crerar, M. Borscik, A. Ronk, and W. Woods, Econ. Geol. 82, 184 (1987).
4.   G. W. McGillivray, D. A. Geeson, and R. C. Greenwood, J. Nucl. Mater. 208, 81 (1994).
5.   L. H. Johnson and D. W. Shoesmith, in *Radioactive Waste Forms for the Future*, W. Lutze and R. C. Ewing (eds.), Elsevier Science Publishing, Amsterdam, The Netherlands (1988) 635 p.
6.   P. A. Finn, J. C. Hoh, S. F. Wolf, M. T. Surchik, E. C. Buck, and J. K. Bates, this volume (1997).
7.   D. J. Wronkiewicz, J. K. Bates, T. J. Gerding, E. Veleckis, and B. S. Tani, Argonne National Laboratory Report ANL-91/11 (1991).
8.   D. J. Wronkiewicz, J. K. Bates, T. J. Gerding, E. Veleckis, and B. S. Tani, J. Nucl. Mater. 190, 107 (1992).
9.   D. J. Wronkiewicz, J. K. Bates, S. F. Wolf, and E. C. Buck, J. Nucl. Mater. (in press).
10.   W. J. Gray and D. M. Strachan, Mater. Res. Soc. Symp. Proc. 212, 205 (1991).

11. R. E. Einziger, L. E. Thomas, H. C. Buchanan, and R. B. Stout, High Level Rad. Waste Mgmt. Proc. Third Inter. Conf. 2, 1449 (1992).
12. B. W. Leslie, E. C. Pearcy, and J. D. Prikryl, Mater. Res. Soc. Symp. Proc. 294, 505 (1993).
13. F. Cesbron, P. Ildefonse, and M-C. Sichere, Mineral. Mag. 57, 301 (1993).
14. W. M. Murphy, Radwaste 2, 44 (1995).

DISCLAIMER